

Synthesis of a New Mesostructured Lamellar Oxovanadium Phosphate Assembled through an $S^+X^-I^0$ Mechanism

Jamal El Haskouri, Saúl Cabrera, Manuel Roca, Jaime Alamo, Aurelio Beltrán-Porter, Daniel Beltrán-Porter, M. Dolores Marcos,* and Pedro Amorós*

Institut de Ciència dels Materials de la Universitat de València (ICMUV), P.O. Box 2085, 46071-València, Spain

Received March 16, 1999

A new lamellar mesostructured oxovanadium(V) phosphate, $(DDAH)_{0.9}(Cl)_{0.9}VOPO_4 \cdot 1.5H_2O$ (DDA = dodecylamine), has been synthesized through a $S^+X^-I^0$ cooperative mechanism using protonated dodecylamine ($DDAH^+$) as structural directing agent. The self-assembling process between 2D- $[VOPO_4]$ moieties and $(DDAH^+ \cdots Cl^-)$ dipolar ion pairs leads to a second-order staged material in which the surfactant molecules are organized in an interdigitated array occupying the gap between double $VOPO_4$ layers defining the inorganic walls. Besides X-ray powder diffraction and TEM observations, results from IR spectroscopy, thermal analysis, and intercalation reactions suggest that the inorganic framework in the title compound has clear similarities with that observed in $VOPO_4 \cdot 2H_2O$.

Introduction

The interest in metal phosphates and related solids having low dimensional (i.e. 1D or 2D) structures is currently increasing as more applications for these materials emerge.^{1,2} Particularly, oxovanadium phosphate chemistry has impressively grown under the attraction of the industrial interest of the $(VO)_2P_2O_7$ catalysts.³ This has resulted in a rich crystal chemistry which is associated, in part, with the ability of vanadium to adopt different coordination polyhedra and to easily accede to various oxidation states.^{4,5} In this context, a great number of new V–P–O solids have been recently identified due to the success of some synthesis tricks that allow the preparation of layered or open frameworks through the incorporation into the resulting networks of inorganic⁶ or organic⁷ species which frequently are referred to, in a broad sense, as templates.⁵

It was in 1992 when a group of scientists of the Mobil company reported on the synthesis of a new family of silica-based mesoporous derivatives (denoted MCM-41) by using large molecular aggregates (surfactants) as “supramolecular tem-

plates”.⁸ Since then, a great effort has been devoted to the preparation of new silica- and non-silica-based mesostructured or mesoporous materials by using similar surfactant-assisted procedures.^{5,9–11} Under this approach, and following our work on oxovanadium phosphates, we have explored the idea that the formation of new low-dimensional V–P–O materials could be favored through self-assembling processes between inorganic fragments and surfactant molecules.

Several vanadium–phosphorus oxide-based mesostructured solids have been prepared up to date using alkyltrimethylammonium salts as surfactants.^{12,13} Thus, hexagonal mesostructured derivatives having the V:P molar ratio of 2:1 were reported by Abe et al.¹² and Doi and Miyake.¹³ Recently, Roca et al.¹⁴ have synthesized, through a cooperative S^+I^- mechanism, new hexagonal mesostructured V–P–O materials (denoted ICMUV-2) in which the bond topology seems to be similar to that in layered oxovanadium phosphates. Moreover, as ICMUV-2 materials have the V:P = 1:1 molar ratio, they are adequate pyrolytic precursors of the $(VO)_2P_2O_7$ catalysts. On the other hand, Doi and Miyake¹³ described also the synthesis of a lamellar mesostructured solid having a V:P molar ratio of, approximately, 1:0.85. This lamellar surfactant-containing solid was prepared using a method similar to that of FSM-16 silicas,¹⁰ i.e. by intercalation of the alkyltrimethylammonium surfactant in the layered $VO(HPO_4) \cdot 0.5H_2O$. In fact, it is this lamellar V:P = 1:0.85 solid which evolves to the above-mentioned hexagonal V:P = 2:1 mesostructured phase when subjected to

* To whom correspondence should be addressed. E-mail: loles.marcos@UV.es; pedro.amoros@UV.es.

(1) Kanazawa, T., Ed. *Inorganic Phosphate Materials*; Elsevier: Tokyo, 1989.
 (2) Clearfield A. *Prog. Inorg. Chem.* **1998**, *47*, 371.
 (3) Centi, G. *Catal. Today* **1993**, *16*, 5.
 (4) Khan, M. I.; Zubieta, J. *Prog. Inorg. Chem.* **1995**, *43*, 1 and references therein.
 (5) Amorós, P.; Marcos, M. D.; Beltrán, A.; Beltrán, D. *Curr. Opin. Solid State Mater. Sci.* **1999**, *4*, 123 and references therein.
 (6) (a) Haushalter, R. C.; Wang, Z.; Thompson, M. E.; Zubieta, J.; O'Connor, C. J. *Inorg. Chem.* **1993**, *32*, 3966. (b) Zhang, Y.; Clearfield, A.; Haushalter, R. C. *J. Solid State Chem.* **1995**, *117*, 157.
 (c) Roca, M.; Marcos, M. D.; Amorós, P.; Alamo, J.; Beltrán, A.; Beltrán, D. *Inorg. Chem.* **1997**, *36*, 3414. (d) Ayyappan, P.; Ramanan, A.; Torardi, C. C. *Inorg. Chem.* **1998**, *37*, 3628.
 (7) (a) Zubieta, J. *Comments Inorg. Chem.* **1994**, *16*, 153 and references therein. (b) Zhang, Y.; Clearfield, A.; Haushalter, R. C. *Chem. Mater.* **1995**, *7*, 1221. (c) Roca, M.; Marcos, M. D.; Amorós, P.; Beltrán, A.; Edwards, A. J.; Beltrán, D. *Inorg. Chem.* **1996**, *35*, 5613. (d) Khan, M. I.; Meyer, L. M.; Haushalter, R. C.; Schweitzer, A. L.; Zubieta, J.; Dye, J. L. *Chem. Mater.* **1996**, *8*, 43.

(8) Beck, J. S.; Vartuli, J. C.; Roth, W. J.; Leonowicz, M. E.; Kresge, C. T.; Schmitt, K. D.; Schlenker, J. L. *J. Am. Chem. Soc.* **1992**, *114*, 10834.

(9) Corma, A. *Chem. Rev.* **1997**, *97*, 2373.

(10) Sayari, A.; Liu, P. *Microporous Mater.* **1997**, *12*, 149.

(11) Ying, J. Y.; Mehnert, C. P.; Wong, M. S. *Angew. Chem., Int. Ed. Engl.* **1999**, *38*, 56.

(12) Abe, T.; Taguchi, A.; Iwamoto, M. *Chem. Mater.* **1995**, *7*, 1429.

(13) Doi, T.; Miyake, T. *Chem. Commun.* **1996**, 1635.

(14) (a) Roca, M.; El Haskouri, J.; Cabrera, S.; Beltrán, A.; Alamo, J.; Beltrán, D.; Marcos, M. D.; Amorós, P. *Chem. Commun.* **1998**, 1883. (b) Roca, M.; El Haskouri, J.; Cabrera, S.; Beltrán, A.; Alamo, J.; Beltrán, D.; Marcos, M. D.; Amorós, P. *Chem. Mater.* **1999**, *11*, 1446.

a subsequent hydrothermal treatment. In any case, it is well-known that the open layered morphology of some oxovanadium phosphates (particularly $\text{VOPO}_4 \cdot 2\text{H}_2\text{O}$),¹⁵ together with their solid-acid character and the presence of readily reducible V(V) ions, makes them versatile hosts for intercalation chemistry.¹⁶ Thus, it should be noted that the intercalation of *n*-alkylamines (that can be thought of as surfactants) in $\text{VOPO}_4 \cdot 2\text{H}_2\text{O}$ and $(\text{V}_{0.14}\text{Nb}_{0.80})\text{OPO}_4 \cdot 2.7\text{H}_2\text{O}$ was reported prior to the discovery of MCM-41 materials.^{17–20} The resulting structures can be described as organic–inorganic composites consisting of alternating stacks of VOPO_4 -like and organic layers.

In this work we report on the synthesis and structural characterization of a new lamellar mesostructured oxovanadium phosphate, $(\text{DDAH})_{0.9}(\text{Cl})_{0.9}\text{VOPO}_4 \cdot 1.5\text{H}_2\text{O}$ (DDA = dodecylamine). As set out below, the ion-mediated $\text{S}^+\text{X}^-\text{I}^0$ self-assembling formation mechanism here proposed is rather unusual, only two examples of synthesis having been previously reported in the literature (MCM-41 silicas prepared under highly acidic conditions and layered zinc phosphate).^{9,21} In contrast, other analogous mechanisms, as $\text{S}^+\text{X}^-\text{I}^+$ or $\text{S}^-\text{M}^+\text{I}^-$, are better documented.^{9–11} We also present a preliminary study of the intercalation reactions of different alcohols in the $(\text{DDAH})_{0.9}(\text{Cl})_{0.9}\text{VOPO}_4 \cdot 1.5\text{H}_2\text{O}$ host lattice.

Experimental Section

Synthesis of $(\text{DDAH})_{0.9}(\text{Cl})_{0.9}\text{VOPO}_4 \cdot 1.5\text{H}_2\text{O}$. The title compound was synthesized according to Jander's procedure,²² which was modified by introducing in the reaction medium DDA (DDA = dodecylamine) as surfactant. The optimized V:P:DDA molar ratio in the mother solution is 1:5.7:1. A typical preparation can be described as follows: 8 mL of concentrated HNO_3 was added to an 1 M aqueous solution of NaH_2PO_4 (18.207 g; 0.114 mol). Then, a 0.75 M solution of NaVO_3 (2.709 g; 0.02 mol) was slowly added while stirring. The resulting solution was red-orange colored, which is characteristic of VO^{3+} cations in water/phosphoric acid media at low pH values.²² Subsequently, an acidified aqueous solution (100 mL of concentrated HCl in 354 mL of water) of DDA (3.780 g; 0.02 mol) was added while stirring at room temperature. Solvent was eliminated by heating at 80 °C until formation of a yellow precipitate. The resulting solid was filtered off, washed repeatedly with water, and air-dried. (Anal. Found: C, 38.0; N, 3.3; H, 8.5; Cl, 8.5; V, 12.9; P, 8.5; water, 7.1. Calcd: C, 38.3; N, 3.2; H, 8.3; Cl, 8.2; V, 13.1; P, 8.0; water, 6.9).

Intercalation Reactions. Insertion of alcohols into the mesostructured host was carried out as follows: 0.2 g of $(\text{DDAH})_{0.9}(\text{Cl})_{0.9}\text{VOPO}_4 \cdot 1.5\text{H}_2\text{O}$ was kept in contact with an excess of alcohol ($\text{CH}_3(\text{CH}_2)_n\text{OH}$; *n* = 0, 1, 2, 3) at room temperature for intervals ranging from a few minutes to ca. 1 h. The resulting yellow-green intercalates were recovered by filtration, washed with water, and air-dried. The amount of intercalated alcohol per V atom was close to one molecule in every case: 1.3 for methanol, 1.1 for ethanol, 1.1 for propanol, and 0.95 for butanol. Intercalation of higher alcohols (such as hexanol or

octanol) occurs very slowly, but even for comparatively long reaction times (several days), we have been not able to obtain single phase products.

Analysis. Vanadium, phosphorus, and chlorine contents were determined by atomic absorption spectrometry (Perkin-Elmer Zeeman 5000), X-ray fluorescence (Philips PW2400 instrument), and electron probe microanalysis (Philips SEM-515 instrument). Water, alcohol, and surfactant contents were determined by CNH elemental and thermogravimetric analyses.

Physical Measurements. X-ray powder diffraction (XRD) patterns were obtained by means of a conventional angle-scanning Seifert 3000TT diffractometer using $\text{Cu K}\alpha$ radiation in steps of 0.04° (2θ) and counting times of 20 s per step. Indexation and profile fitting were performed on patterns collected in steps of 0.02° (2θ) over the angular range $4\text{--}25^\circ$ (2θ) using a counting time of 40 s per step.

Transmission electron microscopy (TEM) images were obtained by means of a Philips CM10 microscope operating at 120 kV with a LaB_6 filament. Specimens were prepared by dispersing the powder in undecane. A drop of this suspension was placed on a holey copper grid covered with a thin carbon film and dried in air. Scanning electron micrographs (SEM) were recorded on a Hitachi 4100FE instrument.

Infrared spectra (IR) were registered on a FT IR Perkin-Elmer 1750 spectrophotometer using dry KBr pellets containing ca. 2% of the sample.

Thermogravimetric analyses were performed using a TGA-7 Perkin-Elmer instrument. Samples were heated to 550 °C at 5°C min^{-1} under flowing air atmosphere. Final solids were characterized by means of X-ray powder diffraction.

Results and Discussion

Synthesis. The synthesis of non-silica-based mesostructured/mesoporous solids usually implies additional difficulties relative to the established procedures for mesoporous silicas: the hydrolysis and condensation processes affecting the inorganic species are, in general, more intricate than those of silicium ions and, also, the structural flexibility of the resulting inorganic fragments (as required for mesostructured phases formation) is lower than that of silicas.^{23,24} Our synthesis approach, which has allowed us to obtain not only the title compound but also other related mesostructured derivatives,^{14,25,26} is based on a simple idea previously discussed in detail:⁵ the resulting framework in the final solid is affected by the nature of the ionic aggregates present in the mother liquor. In this sense, and owing to the complexity of the $\text{V}/\text{H}_3\text{PO}_4/\text{DDA}/\text{water}$ system, we made a first approximation to the problem by independently considering the equilibria involving the organic or inorganic species under standard conditions. Hence, our basic tools to approach the synthesis of the title compound have been the phase diagram of the surfactant and the consideration of the hydrolysis and condensation processes of the inorganic moieties.

Although alkylamines have been usually considered as neutral surfactants when used as "supramolecular templates",^{10,11} it should be noted that both such a neutral character and, consequently, the proposal of S^0I^0 mechanisms only can be valid in a limited range of synthesis conditions. In fact, a long chain primary amine (such as DDA) is a relatively strong base. When work is done at low pH values, the surfactant (amine) molecules

- (15) Tietze, H. R. *Aust. J. Chem.* **1981**, *34*, 2035.
 (16) Kalousova, J.; Votinsky, J.; Benes, L.; Melánova, K.; Zima, V. *Collect. Czech. Chem. Commun.* **1998**, *63*, 1 and references therein.
 (17) Martínez, M.; Jiménez, A.; Moreno, L.; Bruque, S.; Casal, B.; Ruiz, E. *Mater. Res. Bull.* **1985**, *20*, 549.
 (18) Benes, L.; Hyklova, R.; Kalousova, J.; Votinsky, J. *Inorg. Chim. Acta* **1990**, *177*, 71.
 (19) García, A. L.; Moreno, L.; Jiménez, A. *J. Solid State Chem.* **1990**, *87*, 20.
 (20) Morris, M.; Adams, J. M.; Dyer, A. *J. Mater. Chem.* **1991**, *1*, 43.
 (21) (a) Huo, Q.; Margolese, D. I.; Cielsa, U.; Demuth, D. G.; Feng, P.; Gier, T. E.; Sieger, P.; Firouzi, A.; Chmelka, B. F.; Schüth, F.; Stucky, G. D. *Chem. Mater.* **1994**, *6*, 1176. (b) Huo, Q.; Margolese, D. I.; Cielsa, U.; Feng, P.; Gier, T. E.; Sieger, P.; Leon, R.; Petroff, P. M.; Schüth, F.; Stucky, G. D. *Nature* **1994**, *368*, 317.
 (22) Beltrán, D.; Beltrán, A.; Amorós, P.; Ibáñez, R.; Martínez, E.; Le Bail, A.; Férey, G.; Villeneuve, G. *Eur. J. Solid State Inorg. Chem.* **1991**, *28*, 131.

- (23) Baes, C. F.; Mesmer, R. E. *The Hydrolysis of Cations*; John Wiley and Sons: New York, 1976.
 (24) Brinker, C. J.; Scherer, G. W. *Sol–Gel Science. The Physics and Chemistry of Sol–Gel Processing*; Academic Press: San Diego, CA, 1990.
 (25) Cabrera, S.; El Haskouri, J.; Alamo, J.; Beltrán, A.; Beltrán, D.; Mendioroz, S.; Marcos, M. D.; Amorós, P. *Adv. Mater.* **1999**, *11*, 379.
 (26) Cabrera, S.; El Haskouri, J.; Guillem, C.; Beltrán, A.; Beltrán, D.; Mendioroz, S.; Marcos, M. D.; Amorós, P. *Chem. Commun.* **1999**, 333.

must be protonated, and they should be thought of as cationic S^+ surfactants (DDAH⁺ species in the present case). Hence, given that DDA is dissolved in a HCl highly acidified aqueous solution, it is the phase diagram of dodecylammonium chloride which more approximately would adjust it to our synthesis conditions.²⁷ Really, this phase diagram is singular in comparison with those corresponding to other surfactants, such as cetyltrimethylammonium (CTAB), usually employed as “supramolecular templates”. It includes a very small domain ascribed to hexagonally structured DDAH⁺ mesophases, which only could be formed, therefore, under very strict working conditions (temperature and surfactant concentration). On the contrary, the lamellar phase expands over wide ranges of surfactant/water ratio and temperature values. This is not a surprising fact, as far as the occurrence in DDAH⁺ of small headgroups decreases the probability for the formation of rodlike micelles, which are those showing a natural tendency to self-organize in hexagonal packings.^{9,10,21} In short, the small effective size (a_0) of the headgroups in DDAH⁺ will favor packing factor values (g) close to 1 and, hence, the formation of lamellar mesophases.²¹ On the other hand, the surfactant concentration we have used is well below those required for the formation of liquid crystals and even below the critical concentration for micelles formation. Then, a liquid crystal templating mechanism¹¹ can be rejected as that leading to the formation of $(DDAH)_{0.9}(Cl)_{0.9}VOPO_4 \cdot 1.5H_2O$.

Regarding the inorganic subsystem, at the low pH working values at which we have carried out the synthesis of the title compound, the majority species in the starting solution are $VO(H_2O)_5^{3+}$ and $H_2PO_4^{2-}$.²³ As we have previously shown, under these conditions, the successive hydrolysis and condensation reactions can give rise to the formation of $[VOPO_4]_m^{n-}$ 2D anions.^{5,14} In turn, these anions can be thought of as precursors of lamellar, microporous, or mesostructured phosphates having bonding topologies (derived from that $VOPO_4 \cdot 2H_2O$) in which the (OV)-di- $\mu(O,O')PO_4(VO)$ fragment is recognizable as the main structural unit.⁵

All our results indicate that all vanadium atoms in the final solid are V(V), i.e. the vanadium oxidation state does not vary throughout the entire process. Then, the 2D $[VOPO_4]$ fragments should be, although dipolar, uncharged as a whole. Hence, they are not adequate to match by themselves with cationic surfactants as DDAH⁺ entities. It does not seem unlike, therefore, that Cl^- anions, which are present in stoichiometric amounts in the final material (i.e. the DDAH⁺: Cl^- molar ratio in the solid is ca. 1:1), result initially located in the organic–inorganic interface close to the ammonium headgroups to locally compensate charges. In fact, dealing with cationic surfactants, it is well-known that the hydrophobic–hydrophilic interactions, which can give rise to their organization in supramolecular aggregates, result in being more favored when the additional species required to compensate the headgroup charges are relatively small anions (F^- , Cl^-) compared to larger ones (Br^-).²⁸ Thus, it seems reasonable to come to the conclusion that the formation of $(DDAH)_{0.9}(Cl)_{0.9}VOPO_4 \cdot 1.5H_2O$ occurs through a $S^+X^-T^0$ counterion-mediated mechanism. As mentioned above, this seems to be a rather unusual mechanism, as far as the already described small-ion-mediated self-assembling processes between surfactant and inorganic moieties are attributed to ionic (charged) inorganic fragments ($S^+X^-I^+$ and $S^-M^+I^-$ mechanisms) rather than to neutral ones ($S^+X^-T^0$).^{9–11,21}

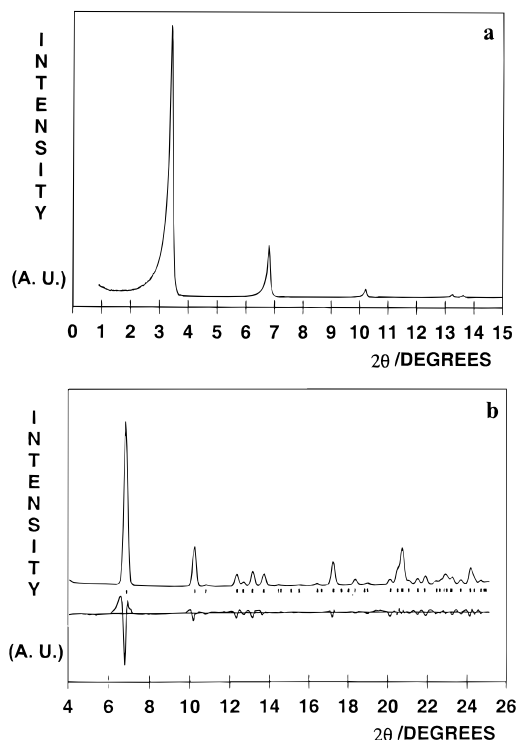


Figure 1. (a) X-ray powder diffraction pattern of $(DDAH)_{0.9}(Cl)_{0.9}VOPO_4 \cdot 1.5H_2O$. (b) Profile refinement of the XRD without structural model (pattern matching) showing the experimental and calculated diffractograms. The difference pattern is at the same scale.

Such a mechanism could be thought of as the result of two main interactions: the Coulombic attraction between the headgroups of the DDAH⁺ molecules and the Cl^- anions, this very likely defining $(DDAH^+ \cdots Cl^-)$ hydrogen-bonded ion pairs, and extended attractive van der Waals forces between these ion pairs and the dipolar 2D $[VOPO_4]$ neutral fragments. In short, it is a templating cooperative $[DDAH^+ \cdots Cl^-]^0 [VOPO_4]^0$ self-assembling process. Taking into account that both ionic and van der Waals interactions are involved as driving forces to the formation of the $(DDAH)_{0.9}(Cl)_{0.9}VOPO_4 \cdot 1.5H_2O$ mesostructure, the proposed mechanism can be viewed as intermediate between ionic and neutral synthesis paths.

Characterization. Electron probe microanalysis shows that the title compound has a constant and well-defined composition with a homogeneous distribution of vanadium, phosphorus, and chlorine atoms in the inorganic framework.

The X-ray powder diffraction (XRD) pattern of $(DDAH)_{0.9}(Cl)_{0.9}VOPO_4 \cdot 1.5H_2O$ is shown in Figure 1a. The fact that a series of equally spaced (d) peaks be observed in the low-angle regime clearly demonstrates the layered structure of the title compound. In consequence,^{29,30} the two major diffraction peaks at 2θ values corresponding to d spacings of 25.97 and 12.99 are assigned to the (001) and (002) reflections, which results in an interlayer spacing of ca. 26 Å. In addition, some weaker but well-resolved peaks are also observed at higher 2θ values. This indicates that the overall layered structure is accompanied by atomic scale ordering and registry of the layers.³⁰ This feature, rarely observed in hexagonal mesostructured materials, is not unusual for lamellar mesophases, and there are some precedents in the literature referred to aluminum and zinc phosphates and iron oxides.^{21,29}

(27) Laughlin, R. G. In *The Aqueous Phase Behaviour of Surfactants*; Academic Press: London 1994; p 125.

(28) Marra, J. J. *Phys. Chem.* **1986**, *90*, 2145.

(29) Oliver, S.; Kuperman, A.; Coombs, N.; Lough, A.; Ozin, G. A. *Nature* **1995**, *378*, 47.

(30) Tolbert, S. H.; Sieger, P.; Stucky, G. D.; Aubin, S. M. J.; Wu, C.; Hendrickson, J. *Am. Chem. Soc.* **1997**, *119*, 8652.

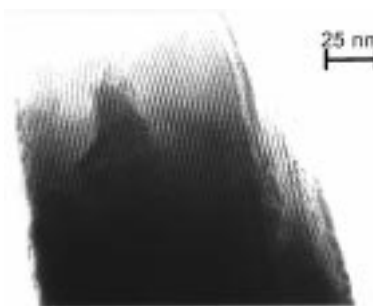
Table 1. X-ray Powder Diffraction Data for (DDAH)_{0.9}(Cl)_{0.9}VOPO₄·1.5H₂O

d_{obs} (Å)	d_{calc} (Å)	hkl	I/I_0 (%)
26.008	26.034	001	100
13.002	13.017	002	20
8.678	8.680	003	4
7.209	7.209	102	1
6.756	6.776	-111	1
6.501	6.508	004	1
6.184	6.179	-112	<1
5.783	5.781	011	<1
5.211	5.207	005	3
4.893	4.895	013	<1
4.374	4.381	-213	2
4.183	4.182	-115	4
4.110	4.108	-202	<1
3.717	3.719	007	2

The XRD pattern of (DDAH)_{0.9}(Cl)_{0.9}VOPO₄·1.5H₂O has been indexed by using the TREOR program. A primitive monoclinic cell with the lattice parameters $a = 10.51$ Å, $b = 7.14$ Å, $c = 26.1$ Å, and $\gamma = 124.1^\circ$ was obtained. Refinement of the cell constants has been accomplished by the Le Bail method using the full pattern without structural model.³¹ A reasonable fit of the experimental data (excluding the largely asymmetric (001) reflection) has been reached in the $P2$ space group (conventional reliability factors: $R_p = 11.5\%$, $R_{wp} = 15.9\%$) leading to the final parameters $a = 10.38(2)$ Å, $b = 7.108(8)$ Å, $c = 26.04(2)$ Å, and $\gamma = 123.4(1)^\circ$. Figure 1b shows the observed and calculated patterns for (DDAH)_{0.9}(Cl)_{0.9}VOPO₄·1.5H₂O. Peaks indexation is shown in Table 1. The parameters defining the inorganic layers are a , b , and γ , and hence, they correspond to nontetragonal [VOPO₄] _{n} layers.

Although, as mentioned above, the effective synthesis conditions initially suggest⁵ that the bond topology in the layers could be similar to that observed in VOPO₄·2H₂O,¹⁵ it is not easy to establish an unambiguous relation between the cell parameters of both solids. Actually, it seems reasonable to assume that the self-assembling of surfactant and VOPO₄ layers (together with the participation of Cl⁻ anions) will induce a significant structural distortion in relation to the original VOPO₄·2H₂O tetragonal cell. The above results suggest a monoclinic distortion in the phosphate layers in such a way that the resulting a parameter is approximately equal to the diagonal of the hypothetical tetragonal cell and the b parameter is about twice the tetragonal one ($a = a_t\sqrt{2}$; $b = 2a_t$). This distortion, together with an additional tilting of the VO₆ and PO₄ polyhedra, would account for the calculated intralayer cell parameters, while the increase of the interlayer c parameter would be related to the interlamellar gap in which the DDAH⁺ and Cl⁻ species must be located.

The layered topology of (DDAH)_{0.9}(Cl)_{0.9}VOPO₄·1.5H₂O is further illustrated by TEM images (see Figure 2), which reveal that all the particles display an homogeneous regular layer disposition, consistent with a monophasic product. The interlamellar distance determined from TEM images (ca. 27 Å) is in good agreement with the XRD data. From these images it is possible to make an estimation of the thickness of the oxovanadium phosphate (ca. 12 Å) and surfactant layers (ca. 15 Å). Then, if the local bond topology in the inorganic layers is similar to that in VOPO₄·2H₂O (see below), the walls in (DDAH)_{0.9}(Cl)_{0.9}VOPO₄·1.5H₂O could be considered as consisting of two VOPO₄ layers located at the usual distance observed in the solid VOPO₄·2H₂O (in fact, on the basis of the structural data reported

**Figure 2.** TEM image of (DDAH)_{0.9}(Cl)_{0.9}VOPO₄·1.5H₂O showing the highly ordered lamellar disposition.

in ref 15, the estimated two-VOPO₄-layers thick in the dihydrate should be 12.2 Å). Regarding the DDAH⁺·Cl⁻ ionic pairs occupying the interlamellar gap, a bilayer disposition of the surfactant molecules can be clearly excluded, taking into account the length of DDAH⁺ molecules (ca. 16.95 Å) and the ionic radii of the Cl⁻ anions (1.81 Å). Hence, it becomes necessary to think about interdigitated dispositions of the DDAH⁺ species. Our calculations shown that such a disposition fits in well with the experimental interlamellar distance if the tilting angle of the aliphatic chains is ca. 40°. This tilting angle value is similar to those described for other lamellar mesostructured derivatives containing both ionic and neutral surfactants as templates.³² Using this tilting angle, and assuming that the cross-section area of an alkyl chain is 19.3 Å,^{2,20} the calculated number of surfactant molecules per each oxovanadium phosphate group should be 1.1–1.2. As can be noted, this value is very close to the experimental one (DDAH⁺:V = 0.9:1). Therefore, all occurs as if the surfactant molecules were organized in a compact packing into the interlayer space.

(DDAH)_{0.9}(Cl)_{0.9}VOPO₄·1.5H₂O shows important differences when compared to the previously described V–P–O materials which contain alkylamines between layers.^{17–20} From the chemical point of view, these last V–P–O compounds were obtained through intercalation (redox reactions) of alkylamines into the inorganic host. In these cases, the intercalation occurs with simultaneous partial reduction of V(V) atoms, and no additional counterion is needed to compensate charges. From the structural point of view, in contrast to the title compound, their inorganic walls are built up from single VOPO₄ layers, and the intercalated organic species are organized in bilayer dispositions that lead to comparatively large interlamellar distances.

SEM micrographs of (DDAH)_{0.9}(Cl)_{0.9}VOPO₄·1.5H₂O (Figure 3) show that the layered morphology is also maintained at the micrometric scale. Thus, the material is built up of prismatic platelike particles with very irregular shape and a constant thickness of ca. 500 nm.

Figure 4 shows the IR spectrum of (DDAH)_{0.9}(Cl)_{0.9}VOPO₄·1.5H₂O. Good band resolution is achieved for vibration modes both of the surfactant and VOPO₄ moieties. Bands due to the VOPO₄ framework are located in the 500–1200 cm⁻¹ range. They are very similar to those appearing in the IR spectrum of VOPO₄·2H₂O,³³ both in energy and relative intensity. Thus, bands at 1035, 1070, and 1140 cm⁻¹ can be assigned to $\nu_{\text{as}}(\text{PO})$ vibration modes of phosphate groups. The intense band appearing at 943 cm⁻¹ and the two shoulders at 850 and 900 cm⁻¹

(31) Larson, A. C.; Von Dreele, R. B. Los Alamos National Laboratory Rep. LA-UR-86-748, 1987.

(32) (a) Yada, M.; Kitamura, H.; Machida, M.; Kijima, T. *Langmuir* **1997**, *13*, 5252. (b) Gao, Q.; Chen, J.; Xu, R.; Yue, Y. *Chem. Mater.* **1997**, *9*, 457.(33) Casañ, N.; Amorós, P.; Ibáñez, R.; Martínez, E.; Beltrán, A.; Beltrán, D. *J. Incl. Phenom.* **1988**, *6*, 193.

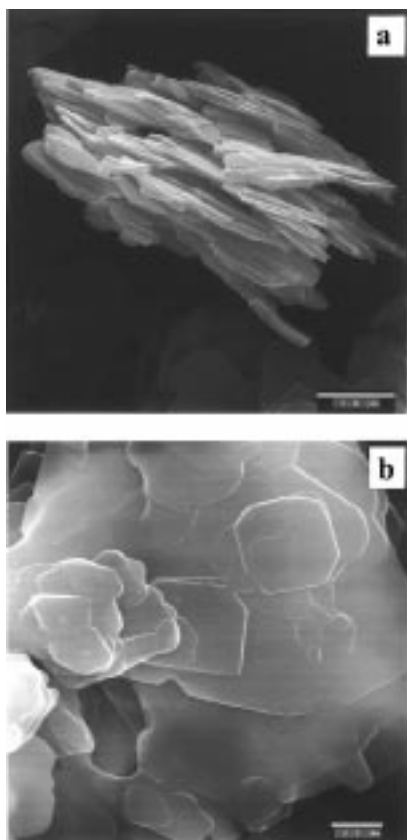


Figure 3. (a) SEM micrographs of $(\text{DDAH})_{0.9}(\text{Cl})_{0.9}\text{VOPO}_4 \cdot 1.5\text{H}_2\text{O}$ in which the characteristic platelike morphology can be observed and (b) perpendicular to the layers view.

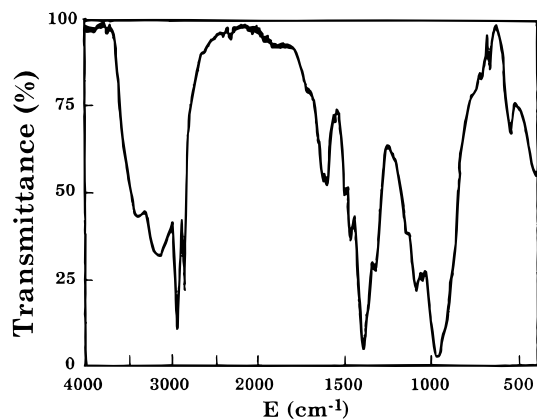


Figure 4. IR spectrum of $(\text{DDAH})_{0.9}(\text{Cl})_{0.9}\text{VOPO}_4 \cdot 1.5\text{H}_2\text{O}$.

can be attributed to $\nu_s(\text{PO})$ vibrations, and a weak band observed at 560 cm^{-1} can be assigned to $\delta_{\text{as}}(\text{OPO})$ vibration modes. On the other hand, the bands observed at 3418 and $1607\text{--}1615\text{ cm}^{-1}$ can be assigned to $\nu(\text{OH})$ and $\delta(\text{HOH})$ vibrations of water molecules. The bending band is clearly split, as occurs in the spectrum of $\text{VOPO}_4 \cdot 2\text{H}_2\text{O}$, which can be related to the presence of two types of H_2O molecules (coordinated and noncoordinated to vanadium atoms). In fact, exception made of the bands associated with the DDAH^+ molecules, the whole aspect of the IR spectrum is similar to that of $\text{VOPO}_4 \cdot 2\text{H}_2\text{O}$.

Regarding the organic molecules, the IR spectrum shows sharp bands in the high-energy range (3139 , 2953 , and 2893 cm^{-1}) that can be assigned to $\nu(\text{NH})$, $\nu_{\text{as}}(\text{CH})$, and $\nu_s(\text{CH})$ vibration modes of DDAH^+ molecules. On the other hand, the region providing the most useful information about the nature of surfactant is that around 1500 cm^{-1} : two bands at 1523 and

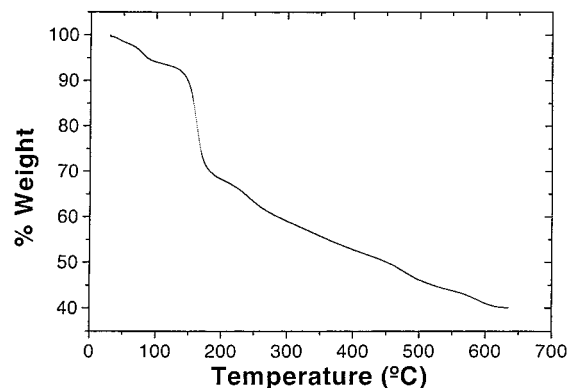


Figure 5. Thermal evolution of $(\text{DDAH})_{0.9}(\text{Cl})_{0.9}\text{VOPO}_4 \cdot 1.5\text{H}_2\text{O}$ under flowing air atmosphere.

1490 cm^{-1} , which can be assigned to $\delta(\text{HNH})$ vibrations of $-\text{NH}_3^+$ species,¹⁹ are clearly observed, this indicating that the amine groups are protonated. In addition, the splitting of these last bands suggests the existence of strong hydrogen-bond interactions.

Figure 5 shows a typical TGA curve (under air flowing atmosphere) of $(\text{DDAH})_{0.9}(\text{Cl})_{0.9}\text{VOPO}_4 \cdot 1.5\text{H}_2\text{O}$. No stable intermediate is evidenced in the course of the thermal evolution. This notwithstanding, three stages can be distinguished along the pyrolytic process: (1) The weight loss of 2.3% observed in the ca. $25\text{--}60\text{ }^\circ\text{C}$ low-temperature range can be attributed to the evolution of loosely bonded (noncoordinated) water molecules. This would agree with the above observation on the basis of IR spectroscopy, and the experimental weight loss would correspond to the evolution of $0.5\text{ H}_2\text{O}$ molecules per V atom. (2) The second weight loss, 4.6%, which is partially superimposed with the previous one, occurs in the ca. $60\text{--}130\text{ }^\circ\text{C}$ temperature range. This weight loss would correspond to the evolution of the remaining water molecules ($1\text{ H}_2\text{O}$ molecule/V atom), which should be coordinated to vanadium atoms. (3) Finally, the last step, which occurs between 130 and $640\text{ }^\circ\text{C}$ with an associated weight loss of 52.1%, corresponds to the evolution of the DDAH^+ and Cl^- species. Under air atmosphere, the solid which result from the thermal treatment is $\beta\text{-VOPO}_4$, as shown by its X-ray powder diffraction pattern. This fact, together with the temperature range in which the two-step dehydration process occurs, supports (as well as the spectroscopic observations above-mentioned) our considerations on the similarities between the title compound and $\text{VOPO}_4 \cdot 2\text{H}_2\text{O}$.¹⁵ On the other hand, the temperature value that initiates removal of the amine (similar to its boiling point) is significantly lower than those observed for the previously reported V–P–O materials which contain intercalated alkylamines ($300\text{--}500\text{ }^\circ\text{C}$).²⁰ In these last, there is a strong ionic interaction between the partially reduced $(\text{VOPO}_4)^{2-}$ layers and the alkylammonium cations. Thus, the present observation should be consistent with our proposal about relatively weak van der Waals interactions between the dipolar $[\text{VOPO}_4]$ layers and the surfactant (or, more adequately, the $[\text{DDAH}^+ \cdots \text{Cl}^-]$ dipole forming ion pairs).

From all the above, it seems reasonable to propose the structural model for $(\text{DDAH})_{0.9}(\text{Cl})_{0.9}\text{VOPO}_4 \cdot 1.5\text{H}_2\text{O}$ that we have represented in Figure 6. It can be thought of as consisting of alternating stacks of inorganic walls (constructed from two VOPO_4 distorted layers) and interdigitated lamellar arrays of DDAH^+ cations. The Cl^- anions should be located at the organic–inorganic interface, close to the surfactant headgroups to locally compensate charges. In short, such a model would respond to a second-order staging behavior, using Whittingham's

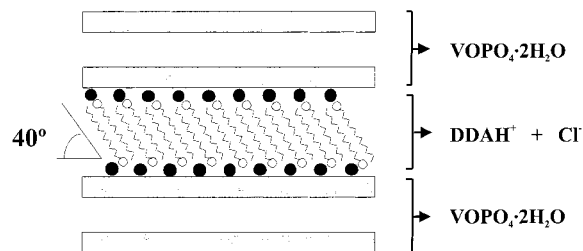


Figure 6. Schematic representation of the structural model proposed for $(\text{DDAH})_{0.9}(\text{Cl})_{0.9}\text{VOPO}_4 \cdot 1.5\text{H}_2\text{O}$: $\sim\text{O} = \text{DDAH}^+$ surfactant molecules; $\bullet = \text{Cl}^-$ counteranions.

terminology,³⁴ which might be related to the effects of elastic coherence strains due to the resulting dipolar character of the guest species.³⁵

Then, we think that, very likely, a formulation such as $\{[(\text{DDAH})(\text{Cl})]_{0.9}[\text{VOPO}_4 \cdot \text{H}_2\text{O}] \cdot 0.5\text{H}_2\text{O}\}_2$ should give a more appropriate description of the title compound than the stoichiometric formula, $(\text{DDAH})_{0.9}(\text{Cl})_{0.9}\text{VOPO}_4 \cdot 1.5\text{H}_2\text{O}$, we have written until now. Actually, there are several interesting points which would result emphasized by means of such a “doubled” formulation, namely (a) the second-order staging behavior, (b) the presence of one water molecule coordinated to each V(V) atom, and (c) the existence of ca. 0.5 loosely bound water molecules which, very likely, are located between the two $\text{VOPO}_4 \cdot \text{H}_2\text{O}$ layers defining the inorganic walls. These last features clearly reflect the above-mentioned similarities between the title compound and $\text{VOPO}_4 \cdot 2\text{H}_2\text{O}$. In an ideal way, we could think about the title compound as resulting from an intercalation process of the guest species ($\text{DDAH}^+ \cdots \text{Cl}^-$ ion pairs) in $\text{VOPO}_4 \cdot 2\text{H}_2\text{O}$, which would originate the elimination of a half of the noncoordinated water molecules of the host—those which would point toward the guest species—as a consequence of the staging behavior due to the dipolar character of the guest species.

Intercalation of Aliphatic Alcohols into $\{[(\text{DDAH})(\text{Cl})]_{0.9}[\text{VOPO}_4 \cdot \text{H}_2\text{O}] \cdot 0.5\text{H}_2\text{O}\}_2$. The intercalates obtained by direct reaction of $\{[(\text{DDAH})(\text{Cl})]_{0.9}[\text{VOPO}_4 \cdot \text{H}_2\text{O}] \cdot 0.5\text{H}_2\text{O}\}_2$ with aliphatic alcohols are yellow or yellow-green solids. This evolution of the color from yellow (host lattice) to light-green is usually observed for V(V) phosphates and related materials and is associated with a certain increase of V(IV) centers that can be expected in alcoholic media. The low-angle diffraction peaks of the intercalates appear shifted to higher 2θ values when compared with those of the host lattice. The intercalates retain the long-range layered order of the matrix, but they do not show any sign of local (atomic scale) order in the walls: their XRD patterns display the peaks assignable to $(00l)$ reflections, but no additional peaks are observed at higher 2θ values.

Intercalation of short-chain alcohols (from methanol to butanol) is a simple reaction for which the reaction time increases (from few minutes to ca. 1 h) as the number of carbon atoms in the chains does. Shown in Figure 7 is a plot of the interlayer distance versus the number of carbon atoms (n_c) in the alkylic chain. As can be noted, the increase of the interlayer distance with n_c shows a typical zigzag evolution. While there is a significant increase in the low-angle peak position when going from $n_c = \text{odd}$ to $n_c = \text{even}$, the changes from $n_c = \text{even}$ to $n_c + 1$ are small. Such an evolution type nicely fits the previous observations concerning the intercalation of alcohols into $\text{VOPO}_4 \cdot 2\text{H}_2\text{O}$ and related solids.¹⁶

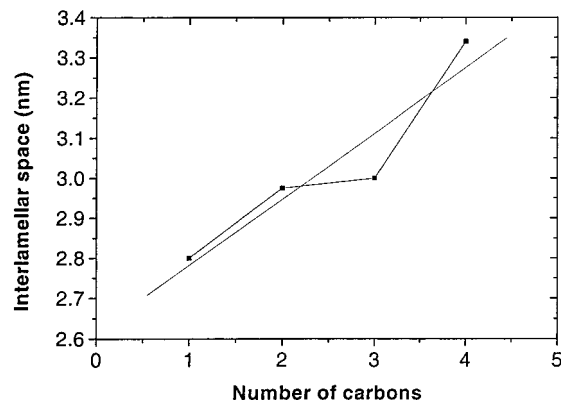


Figure 7. Plot of the interlayer distance versus number of carbon atoms in the intercalated alcohol (from methanol to butanol).

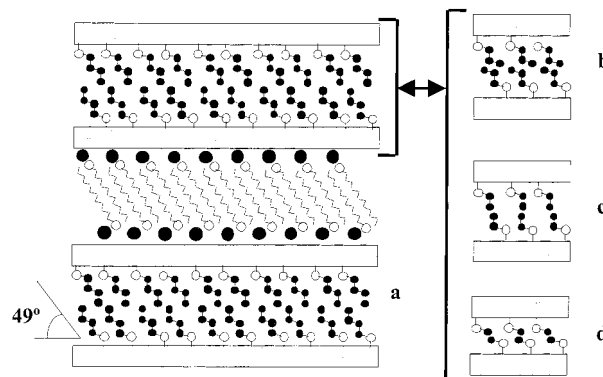


Figure 8. Schematic representation of the short-chain alcohols intercalates: (a) butanol; (b) propanol; (c) ethanol; (d) methanol.

On the other hand, it can be noted also that the ordinate in the origin of the eye-guide dotted line in Figure 7, ca. 26.15 Å, represents the thickness of the original (host lattice) mesostructured material. Interestingly, the interlayer distance increases at a mean rate of 1.92 Å/CH₂. Given that the distance between two adjacent carbon atoms can be expressed as 1.27 Å/CH₂ in an all-trans extended alkyl chain, a noninterdigitated disposition of alcohol molecules in the interlamellar gap would lead to a value of 2.54 Å/CH₂ for the mean “slope”. Both a certain tilting of the aliphatic chains or a partial interdigitation would result, therefore, in “slope” mean values in the 1.27–2.54 Å/CH₂ range.

The typical zigzag evolution of the interlayer distance, as well as the fact that the amount of intercalated alcohol molecules/vanadium atom in $\{[(\text{DDAH})(\text{Cl})]_{0.9}[\text{VOPO}_4 \cdot \text{H}_2\text{O}] \cdot 0.5\text{H}_2\text{O}\}_2$ be half of those entering into $\text{VOPO}_4 \cdot 2\text{H}_2\text{O}$,³⁶ suggests that the alcohol molecules intercalated in $\{[(\text{DDAH})(\text{Cl})]_{0.9}[\text{VOPO}_4 \cdot \text{H}_2\text{O}] \cdot 0.5\text{H}_2\text{O}\}_2$ are arranged as noninterdigitated double layers with a tilt angle of ca. 49° (Figure 8).

Acknowledgment. We thank very much the DGES of the Spanish Ministerio de Educación y Ciencia (Grant PB95-1094) for financial support of this work. J.E.H. and S.C. thank the AECI for doctoral grants.

IC9902931

(36) Actually, we are assuming here a behavior for the intercalated alcohol guest species similar to that previously observed for $\text{VOPO}_4 \cdot 2\text{H}_2\text{O}$. The comparative reduction by a half of the amount of intercalated alcohol molecules is just what could be expected from the $[\text{VOPO}_4 \cdot \text{H}_2\text{O}]$ double layer character of the walls in the title compound. As in the case of $\text{VOPO}_4 \cdot 2\text{H}_2\text{O}$, the incoming of alcohol molecules must result in substitution of both coordinated and noncoordinated water molecules, which in the interlamellar wall space are now ca. half of those found in $\text{VOPO}_4 \cdot 2\text{H}_2\text{O}$.

(34) Whittingham, M. S.; Jacobson, A. J., Eds. *Intercalation Chemistry*; Academic Press: New York, 1982.

(35) Safran, S. A. *Phys. Rev. Lett.* **1980**, *44*, 937.